Optimal Energy Storage Placement in Microgrids

Tuncay Altun, *Student Member, IEEE,* Ramtin Madani, *Member, IEEE,* and Ali Davoudi, *Senior Member, IEEE*

***Abstract*—This paper is concerned with the optimal energy storage placement problem in both AC and DC microgrids to minimize total power generation costs by flattening the generation profile over a given time interval. This planning problem considers diurnal behavior of load profiles as well as the binary variables accounting for the storage location, while respecting physical and operational constraints. A mixed-integer cone programming scheme is developed to tackle the non-convex power flow equations and the complexities posed by binary variables. The proposed optimal energy storage placement is applied to both DC and AC microgrids on modified IEEE 9-bus, 14-bus, and 22-bus systems.**

***Index Terms*—Energy storage, microgrids, optimal placement, planning, scheduling.**

I. Introduction

STORAGE presence in power systems offers a wide range of benefits, including reliability enhancement [1], peak-load shaving [2], voltage regulation [3], load management [4], wind power curtailment [5], or forecast error mitigation [6]. Existing literature have mainly focused on storage operations and sizings, to maximize gains obtained by storage placement in a predetermined location, usually next to a renewable energy source or a large load [7]–[10], and have mainly neglected the effect of location. The optimal storage placement problem boils down to a mixed-integer nonlinear programming model which is computationally challenging due to: i) Non-convex power flow equations, and ii) Binary variables accounting for where to deploy a predetermined number of storage units [11]. These challenges are mostly handled via either a linear approximation of the original problem [12]–[14], or using heuristic methods such as genetic [15] and particle swarm [16] optimization algorithms. The linear approximation assumes a lossless network, and the performance of the heuristic methods depends on some initial conditions [17].

To address non-convexity of power flow equations, various convex relaxation methods have transformed the original problem into surrogates while attempting to preserve an equivalency among them [18], [19]. Convex relaxation methods, second-order cone programming (SOCP) and semi-definite programming (SDP), have been applied to solve the optimal power flow problem in AC microgrids with energy storage [9], [10]. While the optimal storage operation has been studied for AC microgrids, the efforts on the optimal storage placement are rather rare in the literature [20]. Extension to DC microgrids are quite limited to an optimal storage operation [21], [22]. Given that DC microgrids are commonly used in mission-critical applications, optimal energy storage placement is indispensable for planning cost-effective and reliable DC microgrids.

We formulate the optimal energy storage placement problem to minimize the cost of the daily power generation by flattening the generation profile. This problem is formulated as a mixed-integer nonlinear programming (MINLP) that embodies two types of non-convexities due to the quadratic power flow equations and the binary variables to decide the location of storage units. We then relax this problem into a tractable mixed-integer second-order cone programming (MISOCP) that can be solved using standard branch-and-bound solvers. Given a number of energy storage units to be deployed, the proposed framework optimizes the voltage/power set-points of the local converter/inverter or generator controllers, and decides the location of storage units as well as their charge/discharge schedule, while respecting the operational and physical constraints of given power system.

The remainder of this paper has the following organization: Section II defines the preliminaries. Section III details the modeling of DC microgrids with energy storage units, and formulates the optimal storage placement and operation as a MINLP problem. In Section IV, we provide convex relaxation to a MINLP problem through MISOCP relaxation, and discussed its practical extension to an AC microgrid. Section V verifies the resulting MISOCP-relaxed optimal storage placement problems through numerical studies using IEEE benchmarks. Section VI draws the conclusion.

II. Notations

A. General Notations

Herein, vectors are represented by bold small letters, $\boldsymbol{x}$, while bold uppercase letters, $\boldsymbol{X}$, refers to the matrices. The symbol $\mathbf{1}_n$ refers to a vector with the size of n whose elements are 1. The sets of real and complex numbers are symbolized with $\mathbb{R}$ and $\mathbb{C}$, respectively. The $n\times n$ symmetric and hermitian matrices are denoted with $\mathbb{S}^n$ and $\mathbb{H}^n$, respectively. i^{th} row and j^{th} column of a two-dimensional matrix is denoted with (i,j). For a three-dimensional array, (k,ij) refers to k^{th} block, i^{th} row, and j^{th} column. $(\cdot)^\top$ and $(\cdot)^*$, respectively, denote the transpose and conjugate transpose operators. $|\cdot|$ defines both the cardinality of a set or the absolute/magnitude value of a vector/scalar. $[\cdot]$ composes a matrix with diagonal entries from a given vector. $\mathrm{diag}\{\cdot\}$ composes a vertical vector from diagonal elements of a given matrix.

B. Microgrid Notations

This paper considers both DC and AC microgrids. A DC microgrid is defined by a directed graph $\mathcal{H} = (\mathcal{N}, \mathcal{L})$,

This work was supported by the Office of Naval Research under awards N00014-18-1-2186. The authors are with University of Texas, Arlington, TX, 76019, USA (e-mail: tuncay.altun@uta.edu; ramtin.madani@uta.edu; davoudi@uta.edu). The technical content of this work is approved for public release under DCN # 43-7771-21.

with $\mathcal{N}$ and $\mathcal{L}$ as the sets of buses and lines, respectively. Resistive distribution lines connect nodes. Power electronics converters interface energy sources to the grid. Each bus can accommodate an arbitrary number of power electronics converters, loads, or energy storage units. Define $\vec{\boldsymbol{L}}, \overleftarrow{\boldsymbol{L}} \in \{0,1\}^{|\mathcal{L}|\times|\mathcal{N}|}$ as the *from* and *to* line-incidence matrices, respectively. If the line $l \in \mathcal{L}$ starts at bus $k \in \mathcal{N}$, then $\vec{\boldsymbol{L}}_{l,k} = 1$. Similarly, $\overleftarrow{\boldsymbol{L}}_{l,k} = 1$ implies that line l ends at bus k. Matrices $\boldsymbol{Y} \in \mathbb{R}^{|\mathcal{N}|\times|\mathcal{N}|}$, $\vec{\boldsymbol{Y}}, \overleftarrow{\boldsymbol{Y}} \in \mathbb{R}^{|\mathcal{L}|\times|\mathcal{N}|}$ represent the bus-conductance, and the *from* and *to* line-conductance matrices, respectively. The power flow limits over lines are represented with $\boldsymbol{f}^{\max} \in (\mathbb{R} \cup \{\infty\})^{|\mathcal{L}|}$. The incidence matrix for the power converters is defined with $\boldsymbol{G} \in \{0,1\}^{|\mathcal{G}|\times|\mathcal{N}|}$, where $\mathcal{G}$ is the set of power converters. If the power converter $g \in \mathcal{G}$ is located at bus $k \in \mathcal{N}$, then, $\boldsymbol{G}_{g,k} = 1$.

Similarly, an AC microgrid is defined using a directed graph $\tilde{\mathcal{H}}$ with $\tilde{\mathcal{N}}$ and $\tilde{\mathcal{L}}$, denoting the set of nodes and lines, respectively. The vector of complex apparent power generation is denoted by $\tilde{\boldsymbol{s}}_t^{\text{source}} \in \mathbb{C}^{|\tilde{\mathcal{G}}|}$, the vector of complex voltages is represented by $\tilde{\boldsymbol{v}}_t \in \mathbb{C}^{|\tilde{\mathcal{N}}|}$, and $\tilde{\boldsymbol{G}} \in \{0,1\}^{|\tilde{\mathcal{G}}|\times|\tilde{\mathcal{N}}|}$ is the generator incidence matrix. $\tilde{\boldsymbol{d}}_t \in \mathbb{C}^{|\tilde{\mathcal{N}}|}$ gives the vector of nodal load demand. The complex bus, *from*, and *to* admittance matrices are denoted by $\tilde{\boldsymbol{Y}} \in \mathbb{C}^{|\tilde{\mathcal{N}}|\times|\tilde{\mathcal{N}}|}$, and $\vec{\tilde{\boldsymbol{Y}}}$ and $\overleftarrow{\tilde{\boldsymbol{Y}}} \in \mathbb{C}^{|\tilde{\mathcal{L}}|\times|\tilde{\mathcal{N}}|}$, respectively. Similarly, $\vec{\tilde{\boldsymbol{L}}}$, $\overleftarrow{\tilde{\boldsymbol{L}}}\{0,1\}^{|\tilde{\mathcal{L}}|\times|\tilde{\mathcal{N}}|}$ are branch-incidence matrices. The voltage vector $\tilde{\boldsymbol{v}}_t \in \mathbb{C}^{|\tilde{\mathcal{N}}|}$ leads to the matrix $\tilde{\boldsymbol{W}}_t \in \mathbb{H}^{|\tilde{\mathcal{N}}|}$. Other variables shown with a superscript $\tilde{(\cdot)}$ are the AC microgrid counterparts of those described for the DC microgrid.

C. Storage Placement Notations

Optimal storage placement problem aims to minimize the generation cost by flattening the generation profile. It decides voltage/power set-points of converters/inverters, and the location of a predetermined number of storage units, as exemplified in Figure 2, and their charge/discharge schedule, as visualized in Figure 1. Consider the case of a DC microgrid. $t = \{1, 2, 3, ..., |\mathcal{T}|\}$ where $\mathcal{T}$ denotes the length of a diurnal behavior of the aggregated load profile. $\boldsymbol{v}_t \in \mathbb{R}^{|\mathcal{N}|}$ and $\boldsymbol{p}_t^{\text{source}} \in \mathbb{R}^{|\mathcal{G}|}$ are vectors of nodal voltages and power injections into the DC microgrid from the power converters, respectively, at time $t \in \mathcal{T}$. $\boldsymbol{p}_t^{\text{storage}} \in \mathbb{R}^{|\mathcal{N}|}$ are vectors of charge/discharge power of storage units at time $t \in \mathcal{T}$. Herein, the energy transacted over a time-step is converted to power units by dividing it by the length of that time-steps. This helps formulating the problem in terms of power units. $p_{t,sk}^{+}$ and $p_{t,sk}^{-}$ denote charging and discharging rates of a storage unit $s \in \mathcal{S}$ located at bus $k \in \mathcal{N}$ at time $t \in \mathcal{T}$. Herein, $\mathcal{S}$ denotes the set of storage units placed on the grid. $p_{t,k}^{\text{storage}}$ represents the storage level at bus k at time $t \in \mathcal{T}$. Lastly, C_{sk} indicates whether storage s is located at bus k, $C_{sk} = 1$, or not, $C_{sk} = 0$. C_{sk} is the decision variable determined for a given time horizon.

III. Optimal Energy Storage Placement

We formulate the optimal energy storage placement problem as a MINLP problem, and provide its lifted reformulation

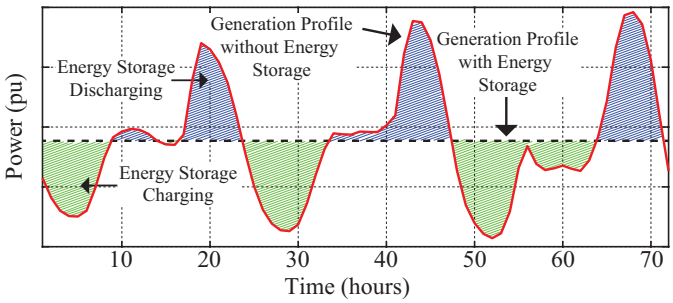

Fig. 1. In the presence of energy storage in a microgrid with sufficient capacity, the proposed algorithm decides the location of storage units, and optimizes their charge/discharge schedule to flatten the generation profile.

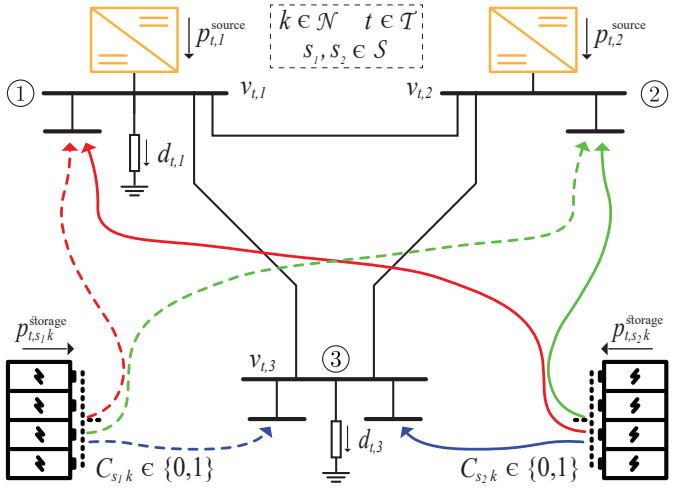

Fig. 2. An example of a three-bus DC microgrid. All the buses are possible candidates to deploy two storage units. Dashed lines present the possible locations for the first storage unit while straight lines show possible locations of the second storage unit. For optimal allocation, one has to decide six binary variables while considering physical and operational constraints and minimizing generation costs.

along with a MISOCP-relaxed version, which is compatible with the state-of-the-art branch-and-bound solvers, enabling the search for binary variables.

A. Energy Storage Modeling

The storage placement in a DC microgrid is formulated as a MINLP problem based on the optimal power flow (OPF) framework, e.g., see [23]. This converts an static OPF problem, with no time coupling, to a scheduling problem that charges a storage unit, when the generation cost is low, and discharges it, when the generation cost is higher. The objective function aims to minimize the total generation costs that can be expressed as a quadratic cost function over $t \in \mathcal{T}$ as

$$\sum_{t\in\mathcal{T}} \left(\boldsymbol{p}_t^{\text{source}\top} [\gamma_t] \boldsymbol{p}_t^{\text{source}} + \boldsymbol{\beta}_t^{\top} \boldsymbol{p}_t^{\text{source}} + \boldsymbol{\alpha}_t^{\top} \mathbf{1}_{|\mathcal{G}|} \right), \quad (1)$$

The vector of power injected/extracted into/from buses at time $t \in \mathcal{T}$ is derived as $\text{diag}\{\boldsymbol{v}_t \boldsymbol{v}_t^{\top} \boldsymbol{Y}^{\top}\} \in \mathbb{R}^{|\mathcal{N}|}$. Similarly, the vectors of *from* and *to* line flows, respectively, are $\text{diag}\{\vec{\boldsymbol{L}} \boldsymbol{v}_t \boldsymbol{v}_t^{\top} \vec{\boldsymbol{Y}}^{\top}\}$ and $\text{diag}\{\overleftarrow{\boldsymbol{L}} \boldsymbol{v}_t \boldsymbol{v}_t^{\top} \overleftarrow{\boldsymbol{Y}}^{\top}\}$, belonging to $\mathbb{R}^{|\mathcal{L}|}$ at time $t \in \mathcal{T}$.

The storage level, at each bus for every time instance. is

$$p_{t,k}^{\text{storage}} = \sum_{s\in\mathcal{S}} \left(p_{t,sk}^{+} - p_{t,sk}^{-}\right), \qquad \forall k \in \mathcal{N}, \tag{2}$$

where $p_{t,sk}^{+}, p_{t,sk}^{-} \geq 0$ are the charge/discharge power received/contributed from/to the node k at time t by the storage unit s. We have $p_{t,k}^{\text{storage}} = 0$ for every $t \in \mathcal{T}$, if no storage unit is placed at bus k. This restriction is imposed by enforcing energy storage unit's upper and lower charging/discharging rates to zero with a binary decision variable as

$$p_{t,sk}^{+} \leq p_{\max;\, s}^{+}\, C_{sk}, \qquad p_{t,sk}^{-} \leq p_{\max;\, s}^{-}\, C_{sk}, \tag{3}$$

If $C_{sk} = 1$, then the storage unit s is placed at node k, and $p_{t,sk}^{+}$ and $p_{t,sk}^{-}$ need to be scheduled by the optimization framework in accordance with the maximum charging/discharging capacity. If $C_{sk} = 0$ then the storage unit s is not located at node k and therefore $p_{t,sk}^{+} = p_{t,sk}^{-} = 0$. The optimal energy storage placement for an infinite time is equivalent to solving the problem for a diurnal cycle given that the law of energy conversion is preserved.

In the following subsections, we formulate the optimal energy storage placement problem as a MINLP that obviates the use of big-M reformulation, in which the constant M is supposed to be properly set: a too small value would have posed a convergence issue, while a too big value would have led to numerical issues [24].

B. Optimal Storage Placement in a DC Microgrid

The lifted, i.e., linearized, version of the optimal storage placement formulation, that optimizes the voltage set-points of converters and locates a pre-determined number of storage units as well as their charge/discharge schedules, can be formulated for a DC microgrid as

$$\text{minimize} \quad \sum_{t\in\mathcal{T}} \left(\boldsymbol{p}_t^{\text{source}^\top}[\boldsymbol{\gamma}_t]\boldsymbol{p}_t^{\text{source}} + \boldsymbol{\beta}_t^\top \boldsymbol{p}_t^{\text{source}} + \boldsymbol{\alpha}_t^\top \mathbf{1}_{|\mathcal{G}|}\right) \tag{4a}$$

$$\text{subject to} \quad \text{diag}\{\boldsymbol{W}_t \boldsymbol{Y}^\top\} + \boldsymbol{d}_t = \boldsymbol{G}^\top \boldsymbol{p}_t^{\text{source}} + \boldsymbol{p}_t^{\text{storage}} \qquad \forall t \in \mathcal{T} \tag{4b}$$

$$|\text{diag}\{\vec{\boldsymbol{L}}\boldsymbol{W}_t\vec{\boldsymbol{Y}}^\top\}| \leq \boldsymbol{f}^{\max} \qquad \forall t \in \mathcal{T} \tag{4c}$$

$$|\text{diag}\{\overleftarrow{\boldsymbol{L}}\boldsymbol{W}_t\overleftarrow{\boldsymbol{Y}}^\top\}| \leq \boldsymbol{f}^{\max} \qquad \forall t \in \mathcal{T} \tag{4d}$$

$$\boldsymbol{p}^{\min} \leq \boldsymbol{p}_t^{\text{source}} \leq \boldsymbol{p}^{\max} \qquad \forall t \in \mathcal{T} \tag{4e}$$

$$(\boldsymbol{v}^{\min})^2 \leq \text{diag}\{\boldsymbol{W}_t\} \leq (\boldsymbol{v}^{\max})^2 \qquad \forall t \in \mathcal{T} \tag{4f}$$

$$p_{t,k}^{\text{storage}} = \sum_{s\in\mathcal{S}} \left(p_{t,sk}^{+} - p_{t,sk}^{-}\right) \qquad \forall k \in \mathcal{N} \quad \forall t \in \mathcal{T} \tag{4g}$$

$$0 \leq p_{t,sk}^{+} \leq p_{\max;\, s}^{+}\, C_{sk} \qquad \forall s \in \mathcal{S} \quad \forall k \in \mathcal{N} \quad \forall t \in \mathcal{T} \tag{4h}$$

$$0 \leq p_{t,sk}^{-} \leq p_{\max;\, s}^{-}\, C_{sk} \qquad \forall s \in \mathcal{S} \quad \forall k \in \mathcal{N} \quad \forall t \in \mathcal{T} \tag{4i}$$

$$\sum_{k=1}^{|\mathcal{N}|} C_{sk} = 1 \qquad \forall s \in \mathcal{S} \tag{4j}$$

$$e_s^{\min} \leq \sum_{t\in\mathcal{T}} \sum_{k\in\mathcal{N}} \left(\mu^+ p_{t,sk}^{+} - \mu^- p_{t,sk}^{-}\right) \leq e_s^{\max} \qquad \forall s \in \mathcal{S} \tag{4k}$$

$$\boldsymbol{W}_t = \boldsymbol{v}_t \boldsymbol{v}_t^\top \qquad \forall t \in \mathcal{T} \tag{4l}$$

$$\text{variables} \quad \boldsymbol{p}_t^{\text{source}} \in \mathbb{R}^{|\mathcal{G}|};\ \boldsymbol{p}_t^{\text{storage}} \in \mathbb{R}^{|\mathcal{S}|};\ \boldsymbol{W}_t \in \mathbb{S}^{|\mathcal{N}|}$$
$$p_{t,sk}^{+},\ p_{t,sk}^{-} \quad \forall s \in \mathcal{S},\ k \in \mathcal{N},\ t \in \mathcal{T}$$
$$C_{sk} \in \{0,1\} \quad \forall s \in \mathcal{S},\ k \in \mathcal{N}$$

where $\boldsymbol{d}_t$ represents the vector of nodal demand at time $t \in \mathcal{T}$, and the vectors $\boldsymbol{p}^{\max}$ and $\boldsymbol{p}^{\min}$ enforce the upper and lower limits of power electronics converters, while the vectors $\boldsymbol{v}^{\max}$ and $\boldsymbol{v}^{\max}$ impose operation boundaries on bus voltages. $p_{\max;\, s}^{+}$ and $p_{\max;\, s}^{-}$ set the maximum charging and discharging rates for every storage unit $s \in \mathcal{S}$. μ^+ and μ^- denote the charging and discharging efficiencies. Equation (4b) imposes the nodal power balances for the entire microgrid. (4c)-(4d) limit the *from* and *to* line power flows. Equation (4j) ensures that a storage unit can only be attached to one bus. The lifted equality constraint in (4l) is nonconvex and needs to be relaxed. Therefore, the lifted equality constraint in (4l) is replaced with the following convex inequalities:

$$W_{t,ii} \times W_{t,jj} \geq |W_{t,ij}|^2 \qquad \forall (i,j) \in \mathcal{L} \quad \forall t \in \mathcal{T}, \tag{5a}$$

$$W_{t,ii} \geq 0 \qquad i \in \mathcal{N} \quad \forall t \in \mathcal{T}. \tag{5b}$$

The resulting MISOCP-relaxed optimal storage placement formulation (4) with the relaxed constraints (5) is compatible with the standard branch-and-bound solvers that decide where to deploy predetermined number of energy storage units.

C. Optimal Storage Placement in an AC Microgrid

The formulation in (4) is extended for AC microgrids as

$$\text{minimize} \quad \sum_{t\in\mathcal{T}} \left(\tilde{\boldsymbol{p}}_t^{\text{source}^\top}[\tilde{\gamma}_t]\tilde{\boldsymbol{p}}_t^{\text{source}} + \tilde{\boldsymbol{\beta}}_t^\top \tilde{\boldsymbol{p}}_t^{\text{source}} + \tilde{\boldsymbol{\alpha}}_t^\top \mathbf{1}_{|\tilde{\mathcal{G}}|}\right) \tag{6a}$$

$$\text{subject to} \quad \text{diag}\{\tilde{\boldsymbol{W}}_t\tilde{\boldsymbol{Y}}^*\} + \tilde{\boldsymbol{d}}_t = \tilde{\boldsymbol{G}}^\top \tilde{\boldsymbol{s}}_t^{\text{source}} + \tilde{\boldsymbol{p}}_t^{\text{storage}} \qquad \forall t \in \mathcal{T} \tag{6b}$$

$$|\text{diag}\{\vec{\tilde{\boldsymbol{L}}}\tilde{\boldsymbol{W}}_t\vec{\tilde{\boldsymbol{Y}}}^*\}| \leq \tilde{\boldsymbol{f}}^{\max} \qquad \forall t \in \mathcal{T} \tag{6c}$$

$$|\text{diag}\{\overleftarrow{\tilde{\boldsymbol{L}}}\tilde{\boldsymbol{W}}_t\overleftarrow{\tilde{\boldsymbol{Y}}}^*\}| \leq \tilde{\boldsymbol{f}}^{\max} \qquad \forall t \in \mathcal{T} \tag{6d}$$

$$\tilde{\boldsymbol{p}}^{\min} \leq \tilde{\boldsymbol{p}}_t^{\text{source}} \leq \tilde{\boldsymbol{p}}^{\max} \qquad \forall t \in \mathcal{T} \tag{6e}$$

$$\tilde{\boldsymbol{q}}^{\min} \leq \tilde{\boldsymbol{q}}_t^{\text{source}} \leq \tilde{\boldsymbol{q}}^{\max} \qquad \forall t \in \mathcal{T} \tag{6f}$$

$$(\tilde{\boldsymbol{v}}^{\min})^2 \leq \text{diag}\{\tilde{\boldsymbol{W}}_t\} \leq (\tilde{\boldsymbol{v}}^{\max})^2 \qquad \forall t \in \mathcal{T} \tag{6g}$$

$$\tilde{p}_{t,k}^{\text{storage}} = \sum_{\tilde{s}\in\tilde{\mathcal{S}}} \left(\tilde{p}_{t,\tilde{s}\tilde{k}}^{+} - \tilde{p}_{t,\tilde{s}\tilde{k}}^{-}\right) \qquad \forall \tilde{k} \in \tilde{\mathcal{N}} \quad \forall t \in \mathcal{T} \tag{6h}$$

$$0 \leq \tilde{p}_{t,\tilde{s}\tilde{k}}^{+} \leq \tilde{p}_{\max;\, \tilde{s}}^{+}\, \tilde{C}_{\tilde{s}\tilde{k}} \qquad \forall \tilde{s} \in \tilde{\mathcal{S}} \quad \forall \tilde{k} \in \tilde{\mathcal{N}} \quad \forall t \in \mathcal{T} \tag{6i}$$

$$0 \leq \tilde{p}_{t,\tilde{s}\tilde{k}}^{-} \leq \tilde{p}_{\max;\, \tilde{s}}^{-}\, \tilde{C}_{\tilde{s}\tilde{k}} \qquad \forall \tilde{s} \in \tilde{\mathcal{S}} \quad \forall \tilde{k} \in \tilde{\mathcal{N}} \quad \forall t \in \mathcal{T} \tag{6j}$$

$$\sum_{k=1}^{|\mathcal{N}|} C_{sk} = 1 \qquad \forall s \in \mathcal{S} \tag{6k}$$

$$\tilde{e}_{\tilde{s}}^{\min} \leq \sum_{t\in\mathcal{T}} \sum_{\tilde{k}\in\tilde{\mathcal{N}}} \left(\tilde{\mu}^+ \tilde{p}_{t,\tilde{s}\tilde{k}}^{+} - \tilde{\mu}^- \tilde{p}_{t,\tilde{s}\tilde{k}}^{-}\right) \leq \tilde{e}_{\tilde{s}}^{\max} \quad \forall \tilde{s} \in \tilde{\mathcal{S}} \tag{6l}$$

$$\tilde{\boldsymbol{W}}_t = \tilde{\boldsymbol{v}}_t \tilde{\boldsymbol{v}}_t^* \qquad \forall t \in \mathcal{T} \tag{6m}$$

$$\text{variables} \quad \tilde{\boldsymbol{p}}_t^{\text{source}} \in \mathbb{R}^{|\tilde{\mathcal{G}}|};\ \tilde{\boldsymbol{p}}_t^{\text{storage}} \in \mathbb{R}^{|\tilde{\mathcal{S}}|};\ \tilde{\boldsymbol{W}}_t \in \mathbb{H}^{|\tilde{\mathcal{N}}|}$$
$$\tilde{p}^{+}_{t,\tilde{s}\tilde{k}},\ \tilde{p}^{-}_{t,\tilde{s}\tilde{k}} \quad \forall \tilde{s} \in \tilde{\mathcal{S}},\ \tilde{k} \in \tilde{\mathcal{N}},\ t \in \mathcal{T}$$
$$\tilde{C}_{\tilde{s}\tilde{k}} \in \{0,1\} \quad \forall \tilde{s} \in \tilde{\mathcal{S}},\ \tilde{k} \in \tilde{\mathcal{N}}$$
$$\tilde{\boldsymbol{s}}_t^{\text{source}} \in \mathbb{C}^{|\tilde{\mathcal{G}}|};\ \tilde{\boldsymbol{q}}_t^{\text{source}} \in \mathbb{R}^{|\tilde{\mathcal{G}}|}$$

where the vector of complex apparent power for all generators, $\tilde{\boldsymbol{s}}_t^{\text{source}} = \tilde{\boldsymbol{p}}_t^{\text{source}} + \mathbf{i}\tilde{\boldsymbol{q}}_t^{\text{source}} \in \mathbb{C}^{|\tilde{\mathcal{G}}|}$, is composed of the active power generation, $\tilde{\boldsymbol{p}}_t^{\text{source}} \in \mathbb{R}^{|\tilde{\mathcal{G}}|}$, and the reactive power generation, $\tilde{\boldsymbol{q}}_t^{\text{source}} \in \mathbb{R}^{|\tilde{\mathcal{G}}|}$. In equation (6), power conservation is accomplished using the power balance equality constraints (6b). Moreover, (6c) and (6d) enforce the line power flows in both directions where $\tilde{\boldsymbol{f}}^{\max}$ instructs the maximum limit. The active and reactive power generation boundaries are imposed in (6e) and (6f), respectively, while voltage levels are restricted with (6g). (6h) determines the storage level at each bus at every time instance. (6i) and (6j) set the maximum charging and discharging rates for storage unit $\tilde{s} \in \tilde{\mathcal{S}}$ upon determination of $\tilde{C}_{\tilde{s}\tilde{k}}$. (6k) ensures that a storage unit can be attached to a single bus.

The optimal storage placement in AC microgrid (6) is the lifted version of its original nonlinear and non-convex formulation. However, the lifted equality constraint in (6m) poses a new sources of non-convexity and needs to be replaced with the following convex inequalities:

$$\tilde{W}_{t,ii} \times \tilde{W}_{t,jj} \geq |\tilde{W}_{t,ij}|^2 \quad \forall (i,j) \in \tilde{\mathcal{L}} \quad \forall t \in \mathcal{T}, \tag{7a}$$
$$\tilde{W}_{t,ii} \geq 0 \quad i \in \tilde{\mathcal{N}} \quad \forall t \in \mathcal{T}. \tag{7b}$$

The equation (6), with (7), leads to a MISOCP-relaxed version of its original nonlinear and non-convex formulation.

IV. Case Studies

A. System Setup

The optimal energy storage placement studies are examined for modified IEEE benchmarks [25] using a PC with a 16-core Xeon processor and 256 GB RAM, CVX v2.1 [26], and the conic mixed-integer solver GUROBI v9.03 [27]. We locate various numbers of energy storage units with different storage capacities for DC and AC microgrids: $e_s^{\max}$ and $\tilde{e}_{\tilde{s}}^{\max}$ set to $\%15$ and $\%25$ of the peak demand, respectively. The charging/discharging rate of a storage unit for DC and AC microgrids, $p^{+}_{t,sk}/p^{-}_{t,sk}$ and $\tilde{p}^{+}_{t,\tilde{s}\tilde{k}}/\tilde{p}^{-}_{t,\tilde{s}\tilde{k}}$, are set to $\%25$ of the maximum storage capacity. The load consumption of each benchmark is spanned for 72-hour period and scaled to comply with the load shape adopted from the Southern California Edison [14]. The proposed optimal storage placement algorithm is applied to the modified IEEE 9-bus, 14-bus, and 22-bus systems. All power values, except for the 14-bus DC microgrid benchmark, are reported in per unit (pu) values.

B. DC Microgrids

IEEE benchmarks are transformed into DC by substituting AC generators with power electronics-interfaced DC source, and modifying distribution lines to be resistive as shown in Figure 3. The proposed method determines the voltage-power set-points of local converter controllers, and decides the location of storage units with their charge/discharge schedule, while respecting the operational and physical constraints of the DC microgrid.

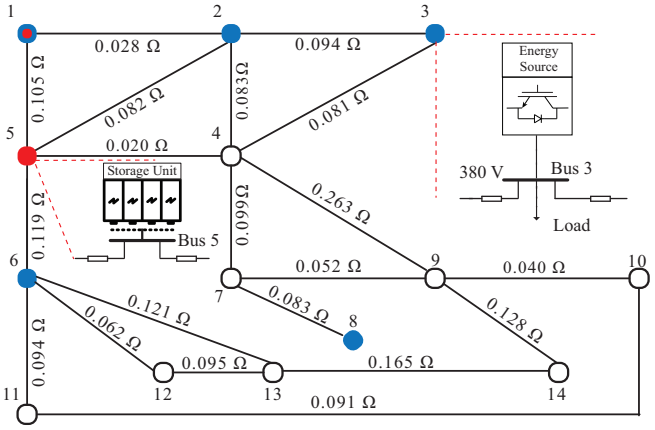

Fig. 3. Modified IEEE 14-bus system with 5 converters that interface sources at buses 1, 2, 3, 6, and 8 shown by ● as well as 2 energy storage units at buses 1 and 5 shown by ●. Note that bus 1, shown by ●, has both a power converter and a storage unit connected.

Modified IEEE 9-bus System: This system includes three loads and three power electronics-interfaced DC sources. In the absence of a storage unit, total power generation cost for a given 72-hour period, as the outcome of (4), is 263778. First, we set the storage capacity of each unit to $\%15$ of the peak demand. Considering (4) for a various number of storage units, e.g., $|S| = 2, 4, 6$, the total generation cost is reduced by flattening the generation profile over the length of 72 hours, as seen in Figure 4. The generation profile, even with 6 storage units $|S| = 6$, has peaks and valleys. By setting the storage capacity of each unit to $\%25$ of their peak demand, the generation profile becomes flat over the given time horizon, see Figure 5.

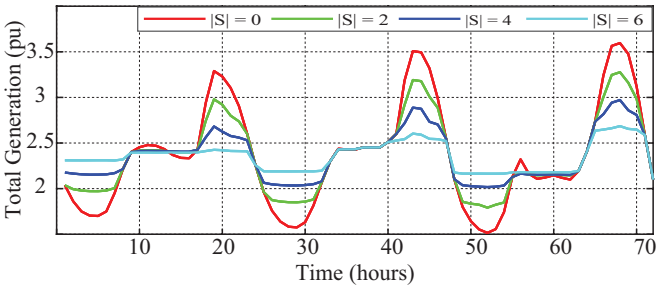

Fig. 4. Total generation profile of the modified 9-bus system, for $|S|$ = 0, 2, 4, 6, when each storage capacity amounts to $\%15$ of the peak demand.

Table I and Table II report the outcomes of (4) in terms of location, cost value, computation time, and the optimality gap for different number of storage units on the modified IEEE 9-bus system. Herein, presence of the storage units in DC microgrids provides up to $\%3.66$ reduction in the total generation cost even in the fixed-pricing strategies with the help of optimally deployed 6 storage units.

Modified IEEE 14-bus System: The peak demand value is 346 kW as shown in Figure 6. The modified IEEE 14-bus system generation profile is observed in the presence of various

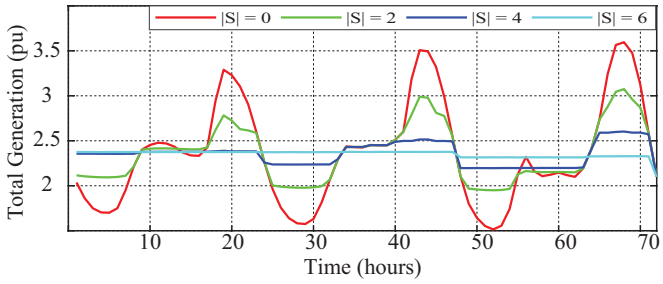

Fig. 5. Total generation profile of the modified 9-bus system, for $|S|$ = 0, 2, 4, 6, when each storage capacity amounts to %25 of the peak demand.

TABLE I
ENERGY STORAGE PLACEMENT (%15 OF THE PEAK DEMAND CAPACITY)

Number of Storage Unit	Storage Location/Unit	Total Cost	Computation Time (s)	Optimality Gap
0	-	263778	3.96	% 100
2	9x2	259195	27.48	% 100
4	5x1, 9x3	256367	184.46	%100
6	5x2, 7x1, 9x3	254859	2540.90	%100

TABLE II
ENERGY STORAGE PLACEMENT (%25 OF THE PEAK DEMAND CAPACITY)

Number of Storage Unit	Storage Location/Unit	Total Cost	Computation Time (s)	Optimality Gap
0	-	263778	3.96	% 100
2	5x1, 9x1	257127	49.74	% 100
4	5x1, 7x1, 9x2	254589	337.40	%100
6	5x2, 7x2, 9x2	254123	3828.25	%100

number of energy storage units. Herein, two different energy storage capacities, $e_s^{\max}$, for 50 kWh and 80 kWh, in which the charging/discharging rates are 12.5 kWh and 20 kWh, i.e., $p_{t,sk}^{+} = p_{t,sk}^{-} = 12.5$ kWh and 20 kWh, respectively. The

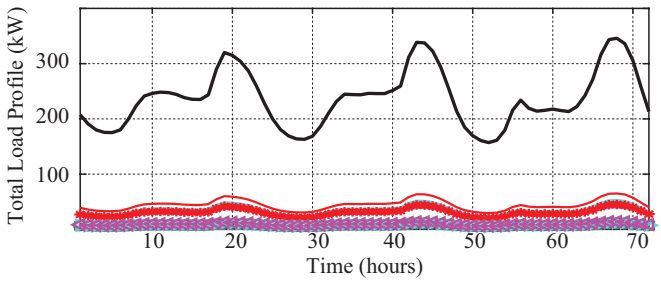

Fig. 6. Load power trajectories and total load in the modified 14-bus system.

modified 14-bus system has five DC sources and ten loads. When there is no storage unit in the microgrid, the total generation cost for a given 72-hour period is 115586. Figure 6 demonstrates the load power trajectories of each load and the total demand profile. Figures 7 and 8 illustrate the energy storage profiles for different energy storage capacities, e.g., %15 and %25 of the peak demand. Figures 9 and 10 show the generation profile for different energy storage capacities.

As seen in Figure 7, the total generation profile is not flat even with 6 storage units. When the storage capacity amounts to %25 of the peak load, as shown in Figure 8, the

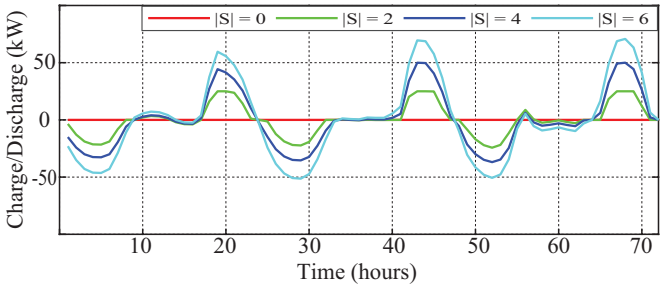

Fig. 7. Energy storage profile of the modified 14-bus system, for $|S|$ = 0, 2, 4, 6, when each storage unit's capacity amounts to %15 of the peak demand.

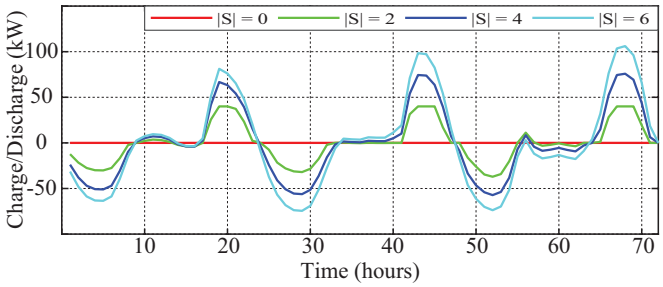

Fig. 8. Energy storage profile of the modified 14-bus system, for $|S|$ = 0, 2, 4, 6, when each storage unit's capacity amounts to %15 of the peak demand.

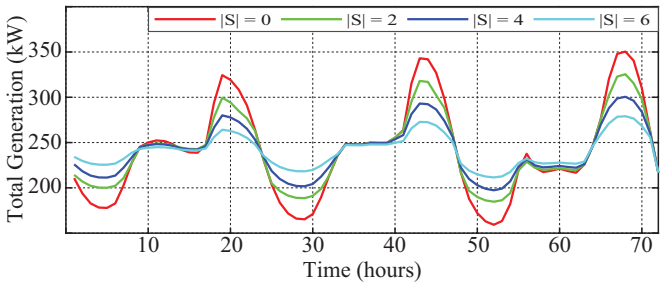

Fig. 9. Total generation profile of the modified 14-bus system, for $|S|$ = 0, 2, 4, 6, when each storage capacity amounts to %15 of the peak demand.

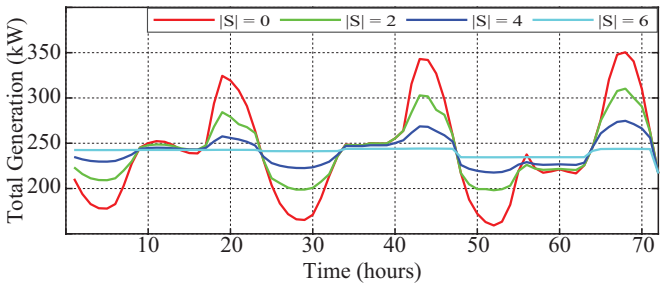

Fig. 10. Total generation profile of the modified 14-bus system, for $|S|$ = 0, 2, 4, 6, when each storage capacity amounts to %25 of the peak demand.

total generation profile becomes fully flatten. Tables III and IV tabulate the results of (4) on the modified IEEE 14-bus system. Per Tables III and IV, total generation cost, even in the fixed-pricing strategy, is reduced by %0.62 with the help of deploying 6 energy storage units. Per Tables III and IV, total generation cost, even in the fixed-pricing strategy, is reduced by %0.62 with the help of deploying 6 energy storage units.

TABLE III
ENERGY STORAGE PLACEMENT ($e_s^{\max} = 50$ KWH)

Number of Storage Unit	Storage Location/Unit	Total Cost	Computation Time (s)	Optimality Gap
0	-	115586	4.16	%0
2	1x1, 4x1	115018	68.47	%0
4	1x2, 4x2	114907	2164.76	%0
6	1x2, 2x1, 5x1, 9x2	114889	16345.26	%0

TABLE IV
ENERGY STORAGE PLACEMENT ($e_s^{\max} = 80$ KWH)

Number of Storage Unit	Storage Location/Unit	Total Cost	Computation Time (s)	Optimality Gap
0	-	115586	4.16	%0
2	1x1, 14x1	115004	138.47	%0
4	1x1, 4x1, 5x1, 6x1	114886	2027.52	%0
6	1x1, 3x1, 4x2, 6x1, 9x1	114875	15887.14	%0

Modified IEEE 22-bus System: This system assumes to have a DC source and 21 loads. Herein, the decision complexity goes up to 132 binary variables. Hence, the computation time to solve (4) for 6 storage units is limited to 24 hours. In the absence of a storage unit, total power generation cost for a given 72-hour period is 683082. Figure 11 demonstrates the generation profile to deploy a different number of storage units. It is observed that the generation profile has not fully flattened yet, even with $|S| = 6$. Upon setting the storage capacity of each unit to %25 of the peak demand, the generation profile becomes flat over the given time horizon, see Figure 12.

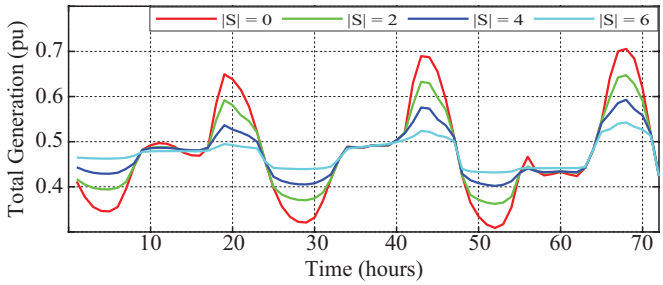

Fig. 11. Total generation profile of the modified 22-bus system, for $|S|$ = 0, 2, 4, 6, when each storage capacity amounts to %15 of the peak demand.

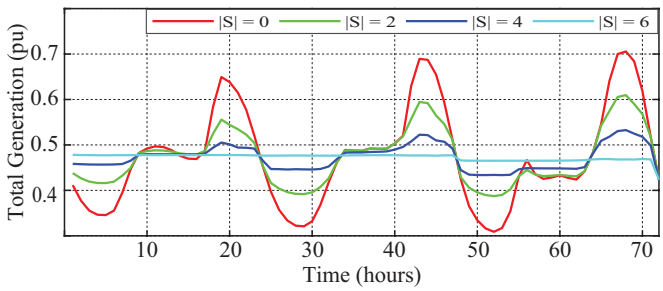

Fig. 12. Total generation profile of the modified 22-bus system, for $|S|$ = 0, 2, 4, 6, when each storage capacity amounts to %25 of the peak demand.

The location, cost, computation time, and optimality gap for different number of storage units on the modified IEEE 22-bus system are reported in the Table V and Table VI. The total generation cost, even in the fixed-pricing strategy, is reduced by up to %0.21 with the help of 6 optimally-deployed storage units. It should be noted in Table VI that the storage placement is not fully completed within the 24 hours timeframe, and has converged to a suboptimal solution.

TABLE V
ENERGY STORAGE PLACEMENT (%15 OF PEAK DEMAND CAPACITY)

Number of Storage Unit	Storage Location/Unit	Total Cost	Computation Time (s)	Optimality Gap
0	-	683082	4.91	%0
2	21x1, 22x1	682350	140.49	%0
4	15x1, 18x2, 21x1	681771	2302.09	%0
6	4x1, 16x3, 21x2	681700	70641.67	%0

TABLE VI
ENERGY STORAGE PLACEMENT (%25 OF PEAK DEMAND CAPACITY)

Number of Storage Unit	Storage Location/Unit	Total Cost	Computation Time (s)	Optimality Gap
0	-	683082	4.91	%0
2	21x2	681885	149.16	%0
4	4x1, 22x3	681604	2739.68	%0
6	1x1, 4x1, 17x1, 18x2, 20x1	681622	86400	%0.21

C. AC Microgrids

Standard IEEE 9-bus System: The standard IEEE 9-bus system consists of three loads and three generators. Figures 13-14 demonstrate the generation profiles, respectively, when the storage capacities are set to %15 and %25 of the peak demand. Each figure includes four different generation profiles depending on the number of storage unit, e.g., $|S|$ = 0, 2, 4, 6. Tables VII and VIII report that the optimal energy storage placement can help reduce the total generation cost by up to %2.16 and %2.35 for the predetermined number of storage units, $|S|$ = 6, and their capacities, %15 and %25, respectively.

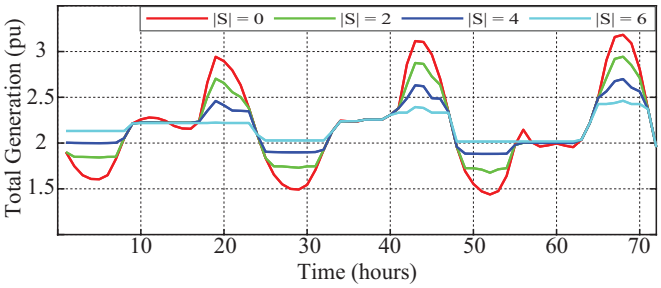

Fig. 13. Total generation profile of the standard 9-bus system, for $|S|$ = 0, 2, 4, 6, when each storage unit's capacity amounts to %15 of the peak demand.

Standard IEEE 14-bus System: The standard IEEE 14-bus system consists of five generators and 10 loads. In the absence of a storage unit, the total generation cost for a given 72-hour period is 357491. Figures 15-16 demonstrate the generation profiles, respectively, when the storage capacities are set to %15 and %25 of the peak demand. It can be observed in Figure 15 that 6 energy storage units, each with the capacity of %25 of peak demand, minimize the peaks and valleys in the

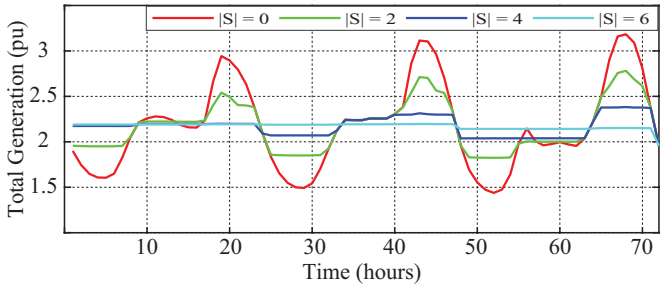

Fig. 14. Total generation profile of the standard 9-bus system, for $|S|$ = 0, 2, 4, 6, when each storage unit's capacity amounts to %25 of the peak demand.

TABLE VII
ENERGY STORAGE PLACEMENT (%15 OF PEAK DEMAND CAPACITY)

Number of Storage Unit	Storage Location/Unit	Total Cost	Computation Time (s)	Optimality Gap
0	-	235677	12.66	%0
2	5x1, 7x1	233172	743.96	%0
4	4x1, 5x1, 9x2	231482	1342.48	%0
6	5x2, 7x2, 9x2	230574	2523.34	%0

TABLE VIII
ENERGY STORAGE PLACEMENT (%25 OF PEAK DEMAND CAPACITY)

Number of Storage Unit	Storage Location/Unit	Total Cost	Computation Time (s)	Optimality Gap
0	-	235677	12.66	%0
2	4x1, 9x1	231965	821.32	%0
4	4x1, 5x1, 7x1, 9x1	230411	1378.48	%0
6	4x1, 5x2, 7x1, 9x2	230126	6302.49	%0

generation profile. Per Tables IX and X, the total generation cost, even in the fixed-pricing strategy, is reduced by up to %1.26 with the help of optimally-deployed 6 storage units.

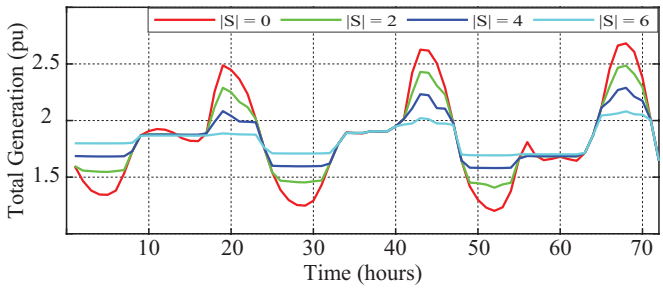

Fig. 15. Total generation profile of the standard 14-bus system, for $|S|$ = 0, 2, 4, 6, when each storage capacity amounts to %15 of the peak demand.

TABLE IX
ENERGY STORAGE PLACEMENT (%15 OF PEAK DEMAND CAPACITY)

Number of Storage Unit	Storage Location/Unit	Total Cost	Computation Time (s)	Optimality Gap
0	-	357491	21.47	%0
2	3x1, 13x1	355506	1013.84	%0
4	3x2, 4x2	354052	16999.90	%0
6	3x3, 5x1, 8x1, 14x1	353216	77341.39	%0

Standard IEEE 22-bus System: This system includes one generator and 21 loads. The computation time is restricted to

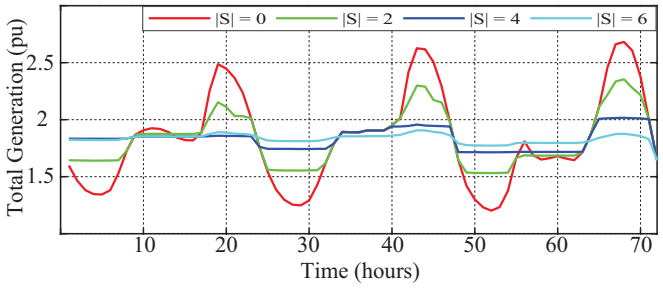

Fig. 16. Total generation profile of the standard 14-bus system, for $|S|$ = 0, 2, 4, 6, when each storage capacity amounts to %25 of the peak demand.

TABLE X
ENERGY STORAGE PLACEMENT (%25 OF PEAK DEMAND CAPACITY)

Number of Storage Unit	Storage Location /Unit	Total Cost	Computation Time (s)	Optimality Gap
0	-	357491	21.47	%0
2	3x1, 9x1	354469	1345.07	%0
4	3x1, 6x1, 7x2	353097	18513.96	%0
6	3x5, 8x1	352991	79786.56	%0

24 hours to solve (6) for 6 storage units. In the absence of a storage unit, total power generation cost for a given 72-hour period is 680945. Figures 17-18 illustrate the generation profile for a various number of storage units. The generation profile with $|S| = 6$ has not fully flattened yet, see Figure 17. Upon setting the storage capacity of each unit to %25 of the peak demand, the generation profile becomes smoother, as shown in Figure 18. As seen in Figure 18, even with greater storage capacities, the generation profile still has the peaks and valleys. This can be helped with an increased number or capacity of the storage units. Tables XI and XII report that the optimal storage placement can help reduce the total generation cost by up to %0.89 and %1.13 for a predetermined number of storage units, $|S|$ = 6, and their capacities, %15 and %25, respectively.

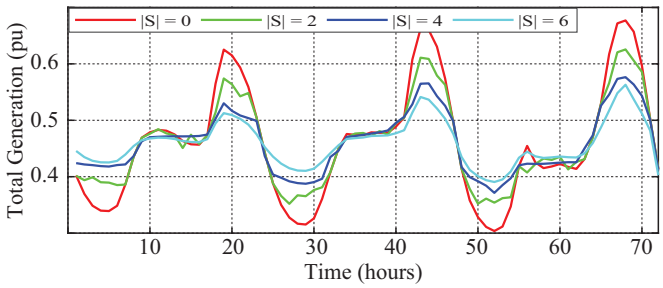

Fig. 17. Total generation profile of the standard 22-bus system, for $|S|$ = 0, 2, 4, 6, when each storage capacity amounts to %15 of the peak demand.

V. CONCLUSION

We examine the effects of energy storage location in a microgrid to minimize total generation costs by flattening the generation profile over time. This method locates a predetermined number of energy storage units, their charge/discharge schedule, and the voltage/power set-points of local converter/inverter or generator controllers, while respecting

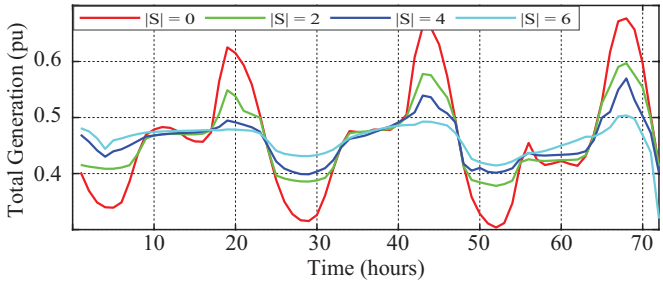

Fig. 18. Total generation profile of the standard 22-bus system, for $|S|$ = 0, 2, 4, 6, when each storage capacity amounts to %25 of the peak demand.

TABLE XI
ENERGY STORAGE PLACEMENT (%15 OF PEAK DEMAND CAPACITY)

Number of Storage Unit	Storage Location/Unit	Total Cost	Computation Time (s)	Optimality Gap
0	-	680945	27.13	%0
2	18x2	678334	856.71	%0
4	5x1, 10x1, 15x1, 16x1	676997	17779.25	%0
6	19x1, 20x5	674895	77341.39	%0

TABLE XII
ENERGY STORAGE PLACEMENT (%25 OF PEAK DEMAND CAPACITY)

Number of Storage Unit	Storage Location/Unit	Total Cost	Computation Time (s)	Optimality Gap
0	-	680945	27.13	%0
2	10x1, 22x1	677454	1583.24	%0
4	1x1, 18x1, 19x2	675113	19459.61	%0
6	1x1, 2x1, 17x1, 18x1, 20x1, 21x1	673221	86400	%0.11

the operational and physical constraints of a given power network. To tackle the non-convex power flow equations and complexities posed by binary variables, a mixed-integer cone programming solution is developed and solved using standard branch-and-bound solvers. Modified or standard IEEE 9-bus, 14-bus, 18-bus, or 22-bus systems are used to study the proposed methodology.

ACKNOWLEDGMENT

We would like to thank Dr. Yujie Tang, from Harvard University, for sharing load profile data with the authors.

REFERENCES

[1] S. Bahramirad, W. Reder, and A. Khodaei, "Reliability-constrained optimal sizing of energy storage system in a microgrid," *IEEE Transactions on Smart Grid*, vol. 3, no. 4, pp. 2056–2062, 2012.

[2] S. X. Chen, H. B. Gooi, and M. Q. Wang, "Sizing of energy storage for microgrids," *IEEE Transactions on Smart Grid*, vol. 3, no. 1, pp. 142–151, 2012.

[3] M. Nick, M. Hohmann, R. Cherkaoui, and M. Paolone, "Optimal location and sizing of distributed storage systems in active distribution networks," in *2013 IEEE Grenoble Conference*, 2013, pp. 1–6.

[4] A. S. A. Awad, T. H. M. EL-Fouly, and M. M. A. Salama, "Optimal ess allocation for load management application," *IEEE Transactions on Power Systems*, vol. 30, no. 1, pp. 327–336, 2015.

[6] F. Luo, K. Meng, Z. Y. Dong, Y. Zheng, Y. Chen, and K. P. Wong, "Coordinated operational planning for wind farm with battery energy storage system," *IEEE Transactions on Sustainable Energy*, vol. 6, no. 1, pp. 253–262, 2015.

[5] Y. Zhang, Z. Y. Dong, F. Luo, Y. Zheng, K. Meng, and K. P. Wong, "Optimal allocation of battery energy storage systems in distribution networks with high wind power penetration," *IET Renewable Power Generation*, vol. 10, no. 8, pp. 1105–1113, 2016.

[7] J. K. Felder and I. A. Hiskens, "Optimal power flow with storage," in *2014 Power Systems Computation Conference*. IEEE, 2014, pp. 1–7.

[8] Y. Levron, J. M. Guerrero, and Y. Beck, "Optimal power flow in microgrids with energy storage," *IEEE Transactions on Power Systems*, vol. 28, no. 3, pp. 3226–3234, 2013.

[9] D. Gayme and U. Topcu, "Optimal power flow with large-scale storage integration," *IEEE Transactions on Power Systems*, vol. 28, no. 2, pp. 709–717, 2012.

[10] L. Fu, K. Meng, B. Liu, and Z. Y. Dong, "Mixed-integer second-order cone programming framework for optimal scheduling of microgrids considering power flow constraints," *IET Renewable Power Generation*, vol. 13, no. 14, pp. 2673–2683, 2019.

[11] H. Pandžić, Y. Wang, T. Qiu, Y. Dvorkin, and D. S. Kirschen, "Near-optimal method for siting and sizing of distributed storage in a transmission network," *IEEE Transactions on Power Systems*, vol. 30, no. 5, pp. 2288–2300, 2014.

[12] E. Sjödin, D. F. Gayme, and U. Topcu, "Risk-mitigated optimal power flow for wind powered grids," in *2012 American Control Conference (ACC)*, 2012, pp. 4431–4437.

[13] C. Thrampoulidis, S. Bose, and B. Hassibi, "Optimal placement of distributed energy storage in power networks," *IEEE Transactions on Automatic Control*, vol. 61, no. 2, pp. 416–429, 2016.

[14] Y. Tang and S. H. Low, "Optimal placement of energy storage in distribution networks," *IEEE Transactions on Smart Grid*, vol. 8, no. 6, pp. 3094–3103, 2017.

[15] G. Carpinelli, G. Celli, S. Mocci, F. Mottola, F. Pilo, and D. Proto, "Optimal integration of distributed energy storage devices in smart grids," *IEEE Transactions on smart grid*, vol. 4, no. 2, pp. 985–995, 2013.

[16] S. Wen, H. Lan, Q. Fu, C. Y. David, and L. Zhang, "Economic allocation for energy storage system considering wind power distribution," *IEEE Transactions on power Systems*, vol. 30, no. 2, pp. 644–652, 2014.

[17] B. Kocuk, S. S. Dey, and X. A. Sun, "New formulation and strong misocp relaxations for ac optimal transmission switching problem," *IEEE Transactions on Power Systems*, vol. 32, no. 6, pp. 4161–4170, 2017.

[18] S. H. Low, "Convex relaxation of optimal power flow—part i: Formulations and equivalence," *IEEE Transactions on Control of Network Systems*, vol. 1, no. 1, pp. 15–27, 2014.

[19] J. Lavaei and S. H. Low, "Zero duality gap in optimal power flow problem," *IEEE Transactions on Power Systems*, vol. 27, no. 1, pp. 92–107, 2011.

[20] S. Bose, D. F. Gayme, U. Topcu, and K. M. Chandy, "Optimal placement of energy storage in the grid," in *2012 IEEE 51st IEEE Conference on Decision and Control (CDC)*. IEEE, 2012, pp. 5605–5612.

[21] M.-H. Wang, S.-C. Tan, C.-K. Lee, and S. Hui, "A configuration of storage system for dc microgrids," *IEEE Transactions on Power Electronics*, vol. 33, no. 5, pp. 3722–3733, 2017.

[22] B. Papari, C. S. Edrington, T. V. Vu, and F. Diaz-Franco, "A heuristic method for optimal energy management of dc microgrid," in *2017 IEEE Second International Conference on DC Microgrids (ICDCM)*, 2017, pp. 337–343.

[23] T. Altun, R. Madani, A. P. Yadav, A. Nasir, and A. Davoudi, "Optimal reconfiguration of dc networks," *IEEE Transactions on Power Systems*, vol. 35, no. 6, pp. 4272–4284, 2020.

[24] M. Cococcioni and L. Fiaschi, "The big-m method with the numerical infinite m," *Optimization Letters*, pp. 1–14, 2020.

[25] R. Christie, "Power systems test case archive, university of washington," *Electrical Engineering. https://www2. ee. washington. edu/research/pstca*, 2000.

[26] M. Grant and S. Boyd, "Cvx: Matlab software for disciplined convex programming, version 2.1," 2014.

[27] I. Gurobi Optimization, "Gurobi optimizer reference manual," 2018.